

Fabrication and Clinical Evaluation of a Novel 3D printed Hydroxyapatite/Polycaprolactone Composite (Novel 3DP HA/PCL) for Maxillary Sinus Augmentation: A Preliminary Study

Poommarin Thammanoonkul¹ Suwit Limpattamapanee² Faungchat Thammarakcharoen³
Jintamai Suwanprateeb^{3,4} Borvornwut Buranawat^{5*}

Abstract

Objective: To fabricate a 3DP hydroxyapatite/polycaprolactone composite graft material and assess its clinical efficacy in maxillary sinus augmentation through a preliminary assessment of bone density changes over a one-year period, compared to deproteinized bovine bone mineral graft.

Methods: A 3DP hydroxyapatite/polycaprolactone (HA/PCL) composite was fabricated using 3D printing of calcium sulfate-based material, followed by phase transformation and PCL infiltration. The composite was characterized through SEM, XRD, micro-CT, and compression testing. In a clinical study, 3DP HA/PCL composite material was compared with deproteinized bovine bone graft in sinus augmentation procedures. Cone-beam computed tomography (CBCT) was used to measure bone density at baseline, 6 months, and 1-year post-operation.

Results: SEM and micro-CT analyses revealed that the 3DP HA/PCL composite exhibited a highly porous, three-dimensional architecture with HA crystals combined with PCL. The microstructure was characterized by a mixture of spherical and irregular-shaped particles with 60.67% porosity. Compression testing demonstrated that the 3DP HA/PCL composite granules had a compressive load resistance of 7.55 ± 1.71 N. The calculated compressive strength of the granule was approximately 2.4 MPa. CBCT analysis of bone density changes revealed distinct patterns between the two groups. Significant differences in graft bone density were observed in the control group at all time points ($P < 0.05$), while the 3DP HA/PCL group demonstrated no significant changes ($P < 0.3831$). However, between 6 months to 1 year, the 3DP HA/PCL group exhibited an increased bone density gain trend similar to the rate observed in the xenograft group. At 1 year, the increase in bone density from T1 to T3 was significant in both the control and test groups. These findings indicate that while 3DP HA/PCL grafts initially increase bone density more slowly than xenografts, they demonstrate a more pronounced gain in the later phase compared to the early phase.

Conclusion: Based on the promising preliminary results from the sinus augmentation study, 3DP HA/PCL composite demonstrates potential as an alternative bone graft material to deproteinized bovine bone mineral.

Keywords: Polycaprolactone, Augment bone graft, Hydroxyapatite, Bone density

Received Date: Aug 05, 2024

Revised Date: Oct 24, 2024

Accepted Date: Nov 11, 2024

¹Division of Periodontics and Implant Dentistry, Faculty of Dentistry, Thammasat University, Pathum Thani, 12120, Thailand.

²Nakhon Ratchasima Provincial Public Health Office, Nakhon Ratchasima, 30280, Thailand.

³Biofunctional Materials and Devices Research Group, National Metal and Materials Technology Center, National Science and Technology Development Agency, Pathum Thani, 12120, Thailand.

⁴Center of Excellence in Computational Mechanics and Medical Engineering, Thammasat University, Pathum Thani, 12120, Thailand.

⁵Department of Implantology, Faculty of Dentistry, Thammasat University, Pathum Thani, 12120, Thailand.

(*corresponding author)

Introduction

Dental implants have emerged as an effective treatment for patients with partial or complete edentulism. However, tooth loss triggers both horizontal and vertical bone resorption. The alveolar ridge volume decreases by 25% within the first year post-extraction, while its width diminishes by 40-60% over the initial three years (1,2). This significant bone loss poses challenges for implant placement, often necessitating bone augmentation procedures. The posterior maxilla, particularly in the premolar-molar region, presents unique challenges for dental implant placement. This area is characterized by low bone density, typically classified as D3-D4 type (150-850 Hounsfield Units) according to Misch's 1988 classification (3). Such bone quality features thin porous cortical bone and fine trabeculae, which can compromise implant stability. Furthermore, the natural pneumatization of the maxillary sinus often results in limited vertical bone height, further complicating implant procedures in this region. To address insufficient bone volume in the posterior atrophic maxilla, various surgical techniques have been developed for maxillary sinus augmentation. Lateral sinus augmentation is indicated when the residual alveolar ridge height is less than 4 mm. This technique has demonstrated superior predictability and reliability for bone augmentation in the posterior maxilla. Extensive literatures support its efficacy and long-term success in preparing sites for dental implant placement, with high reported implant survival rates (4,5). The maxillary sinus, however, exhibits significant anatomical variability. Sinus septa, for instance, are present in 25-31.7% of maxillary sinuses. Additionally,

the proximity of posterior superior alveolar arteries to the surgical site can pose challenges. These anatomical variations may lead to potential complications during sinus augmentation procedures, necessitating careful preoperative assessment and surgical planning (6). Cone-beam computed tomography (CBCT) analysis provides crucial information that helps reduce complications and optimize treatment plans for both sinus augmentation and implant placement. This imaging modality enables precise evaluation of anatomical variations and vital structures, enhancing surgical predictability and safety. Bone grafting materials play a crucial role in maxillary sinus augmentation procedures, significantly enhancing outcomes compared to augmentation without grafts (7). In the absence of bone grafts, the elevated sinus membrane may collapse, resulting in insufficient bone formation and compromised implant stability. Grafting materials serve multiple functions: they maintain the elevated space and provide a scaffold for new bone growth.

A variety of options are available, including autografts, allografts, xenografts, and alloplasts. While autogenous bone is considered the gold standard for reconstruction due to its osteogenic properties, it is associated with a higher resorption rate. In recent years, xenografts have gained popularity in maxillary sinus augmentation, particularly deproteinized bovine bone (8,9). These materials exhibit excellent osteoconductive properties and a slow resorption rate, effectively maintaining space and volume until new bone formation occurs. However, the search for ideal grafting materials in maxillary sinus augmentation continues, driving ongoing research and development in this field.

In addition to allografts and xenografts, alloplastic or synthetic bone grafts have gained considerable popularity in the field of bone augmentation. These synthetic bone grafts, derived from biomaterials, offer an alternative to human or animal-derived products. Hydroxyapatite (10), a key component in many alloplasts, has been utilized in bone repair for years due to its similarity to the inorganic component of natural bone. As a bioceramic material, hydroxyapatite exhibits several advantageous properties: biocompatibility, bioactivity, non-immunogenicity, and excellent osteoconductivity. However, hydroxyapatite's brittleness and limited mechanical strength may make it unsuitable for use in load-bearing area (11-13).

Several studies have investigated the addition of biodegradable polymers, such as polycaprolactone (PCL), to hydroxyapatite (HA) to improve the mechanical properties of bone substitute materials, resulting in HA/PCL composites. (14,15) Polycaprolactone (PCL) exhibits exceptional toughness and biocompatibility (16). It degrades more slowly and has higher fracture energy compared to other biodegradable polymers, while producing less acidic and less toxic degradation products (17). The 3DP HA/PCL composite leverages the advantages of both materials. The HA component provides osteoconductive properties to support bone ingrowth, while the PCL phase improves the mechanical integrity of the graft (15).

The search for optimal grafting materials for maxillary sinus augmentation remains an active area of research. To address this need, a 3D printed hydroxyapatite/polycaprolactone (3DP HA/PCL) composite material has been developed. (18) This 3DP HA/PCL composite has undergone

both in vitro (19) and in vivo (20) testing to assess its biofunction, biosafety, and biocompatibility.

This study has two primary objectives, to comprehensively characterize the 3DP HA/PCL composite material and to evaluate its clinical efficacy in maxillary sinus augmentation compared to the widely used deproteinized bovine bone mineral (DBBM) graft. This comparison will be conducted through a preliminary assessment of bone density changes over a one-year period, providing insights into the material's performance in a clinical setting.

Materials and Methods

The National Metal and Materials Technology Center (MTEC) manufactured a custom 3DP HA/PCL granules using a low-temperature technique (21) with the advantage of the bioresorption ability of HA, allowing for simultaneous bone formation (22,23) and enhancing the mechanical property by infiltration with the biodegradable synthetic polymer (15,21).

These 3DP HA/PCL granules were fabricated through a multi-step process. Initially, a powder-based binder jetting three-dimensional printing machine (Projet160, 3D Systems, USA) was used to fabricate structures using calcium sulfate-based powder (Visijet PXL core, 3D Systems, USA). These three dimensional printed specimens then underwent a phase transformation to 3D printed hydroxyapatite (3DP HA) by soaking in 1 M disodium hydrogen phosphate solution (Sigma Aldrich, USA) at 100°C for 48 hours. Following this transformation, the specimens were thoroughly cleaned overnight in deionized water and subsequently dried at 80°C for 4 hours.

To produce the final 3DP HA/PCL composite, the 3DP HA structures were impregnated with polycaprolactone. This was achieved by soaking the 3DP HA in a 50% w/w solution of polycaprolactone (Sigma Aldrich, Mn~10,000) in N-methylpyrrolidone (TSquare Synergy (Thailand) Co., Ltd, Thailand) at 50°C for 15 minutes.

The infiltrated samples were then transferred into the bottle which contained a 9:1 ratio of N-methylpyrrolidone and deionized water and the bottle was shaken continuously for 45 seconds. The specimens were taken out, cleaned in deionized water for 24 hours and dried at room temperature for 48 hours. Then packed in the glass vial and sterilizable pouch and sterilized by ethylene oxide gas. (Figure 1)

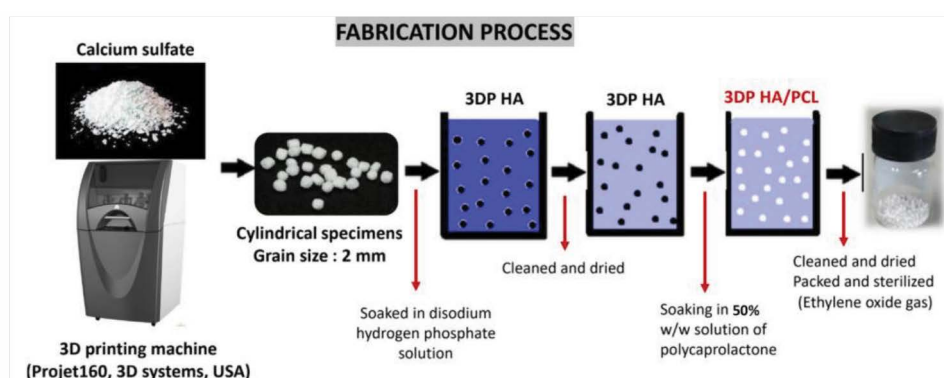


Fig.1 Schematic of the fabrication process for 3D printed hydroxyapatite/polycaprolactone (3DP HA/PCL) composite material. The process begins with the generation of hydroxyapatite (HA) particles, which are then soaked in a polycaprolactone (PCL) solution.

Characterization of the 3DP HA/PCL composite material

The physicochemical properties of the 3DP HA/PCL composite material were comprehensively characterized using a multi-modal approach. X-ray powder diffraction (XRD) analysis was performed using a TTRAX III (Rigaku, USA) with Cu source K α line focused radiation ($\lambda = 0.15406$ nm) operating at 300 mA and 50 kV to elucidate the crystalline structure of the composite. Surface topography was examined using scanning electron microscopy (SEM) with a JCM 6000 (JEOL, Tokyo, Japan). This technique provided high-resolution images of the material's surface features and morphology.

To obtain a three-dimensional representation of the composite's internal structure, microCT scanning was employed using a Skyscan 1275 system (Bruker micro-CT, Kontich, Belgium). The accompanying Skyscan 1275 control software was utilized for image acquisition and subsequent 3D data analysis. This non-destructive imaging technique allowed for detailed visualization and quantification of the material's spatial characteristics.

Compression load resistance of individual granules was performed by using a universal testing machine (Instron 55R4502, Instron, USA) at the crosshead speed of 1 mm/min at $23 \pm 2^\circ\text{C}$

and 50 ± 5 % RH. The maximum load before breakage was recorded and ten replicates were done.

Clinical study

This preliminary study was a prospective single-blinded randomized controlled clinical trial to evaluate the clinical efficacy of the 3DP HA/PCL composite material (Test group: 2.0 mm, MTEC, NSTDA, Thailand) compared to commercial xenograft (Control group: Straumann® Xenograft, 1.0-2.0 mm, Institut Straumann AG, Switzerland) for maxillary sinus augmentation. The study follows CONSORT and Helsinki guidelines, was approved by Thammasat University's Human Research Ethics Committee (COA number 053/2564), and registered on the Thai Clinical Trials Registry (TCTR20210622003)

This study enrolled 22 patients with 24 maxillary sinuses requiring lateral sinus augmentation for 1-2 dental implants, with residual alveolar bone height ≤ 4 mm in upper premolar-molar area, observed on CBCT image. Patients were aged 18-70 years and classified as ASA 1-2. All participants understood the protocols and signed informed consent before enrollment. None had a history of allergy or hypersensitivity to study materials or previous sinus pathology. Exclusion criteria included smoking over 10 cigarettes per day, medical conditions affecting bone and soft tissue healing (e.g., bone disease, osteoporosis, uncontrolled diabetes), and inability to take impressions (both conventional and digital) or CBCT. Sample size is calculated from the equation considering a 20% drop out rate. (24) The randomization and allocation are assigned to the control/test group by a sequentially numbered, sealed envelope protocol. The surgeon opened the sealed envelope before graft placement.

Surgical Procedure

All procedures were performed under local anesthesia using 4% articaine with epinephrine 1:100,000. A mucoperiosteal trapezoidal flap was raised, initiated by a crestal incision followed by two vertical releasing incisions. The flap was gently elevated from the native bone tissue to allow complete visualization of the defect and surrounding bone. Osteotomies on the lateral wall of the maxillary sinuses were performed using the DASK kit (Dentium, Korea). Subsequently, the sinus membrane was elevated, and bone grafting material was packed at the base of the sinus according to the allocated group. Valsalva maneuvers were conducted throughout all stages of sinus floor elevation to ensure membrane integrity.

Following graft placement, the lateral window access was covered with a resorbable collagen membrane (Lyoplant®, Aesculap, USA). Wound closure was achieved using VICRYL® 4-0 and Nylon ETHILON® 5-0 sutures.

Radiographic protocol

Cone-beam computed tomography (CBCT) imaging was performed with a 3D Accuitomo 170 scanner (J. Morita Manufacturing Corp) and taken immediately after maxillary sinus augmentation (T1), 6 months after maxillary sinus augmentation and before implant placement (T2) and 1 year after maxillary sinus augmentation and after prosthesis loading (T3). CBCT images were processed in DICOM file and three-dimensionally (3-D) reconstructed using software (i-Dixel One Volume Viewer, version 2.8.0, J. Morita Manufacturing Corp.) to evaluate bone density.

Clinical and radiographic evaluation

All patients were evaluated by a single examiner one day after sinus augmentation surgery, followed by a two-week post-operative check-up. Subsequently, regular follow-up examinations were conducted at three, six, and twelve months post-surgery to monitor healing progress and assess long-term outcomes.

Bone density, expressed in Hounsfield Units (HU), was measured using the initial floor of maxillary sinus prior to augmentation as a baseline reference. Measurements were taken at two vertical levels: 3 mm and 5 mm superior to this baseline, along the implant axis. At each level, four measurement points were established

around the implant, resulting in a total of eight measurement points. These points were determined by extending horizontal lines perpendicular to the implant axis, 3 mm to each side.

The measurement points were designated as follows:

- At 3 mm above baseline: HU_{B3} (buccal), HU_{Pa3} (palatal), HU_{M3} (mesial), HU_{D3} (distal)
- At 5 mm above baseline: HU_{B5} (buccal), HU_{Pa5} (palatal), HU_{M5} (mesial), HU_{D5} (distal)

Radiographic assessments were performed at three time points (T1, T2, T3) for each patient (Figure 2). The mean values of these measurements (HUA_v) were used for statistical analysis.

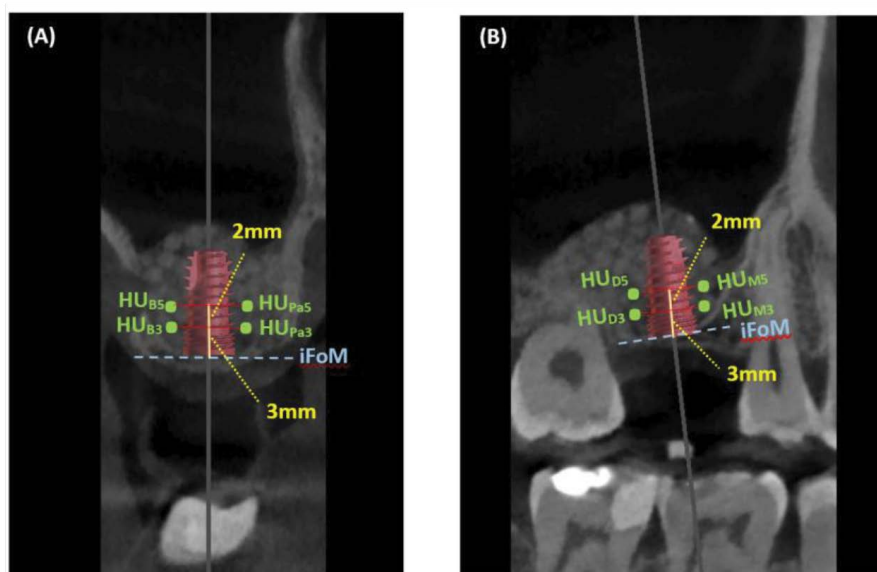


Fig.2 Quantitative analysis of grafted bone density using CBCT data. (A) Bucco-palatal view: This image shows the measurement points for grafted bone density at the buccal and palatal aspects. Measurements were taken at level 3 mm (HUB3, HUPa3) and 5 mm (HUB5, HUPa5) superior to the initial floor of the maxillary sinus (iFoM). The iFoM represents the baseline sinus floor position at T0, prior to augmentation. **(B) Mesio-distal view:** This image demonstrates the measurement points for grafted bone density at the mesial and distal aspects. Similarly, measurements were taken at level 3 mm (HUM3, HUD3) and 5 mm (HUM5, HUD5) superior to the initial floor of the maxillary sinus.

Statistical Analysis

All data were analyzed using descriptive statistics with GraphPad Prism 10.2.2. The significance level was set at $\alpha = 0.05$. Results are presented as mean \pm standard deviation (SD). Given the normal distribution of data, unpaired t-tests were used to compare mean bone density at each time point (T1, T2, T3) between test and control groups. Changes in mean grafted bone density over time within each group were assessed using ANOVA.

Results

Characterizations of 3DP HA/PCL composite

X-ray diffraction (XRD) analysis confirmed the successful incorporation of polycaprolactone (PCL) into the hydroxyapatite (HA) to produce 3DP HA/PCL composite (Figure 3A). The XRD pattern exhibited a combination of characteristic peaks for both PCL and HA. Distinctive PCL peaks were observed at 2θ values of 15.3° , 21.4° , and 23.8° . Concurrently, the presence of HA was evidenced by peaks at 2θ values of 25.8° , 31.6° , 32.14° , 32.8° , and 34.01° . This composite diffraction pattern demonstrates the coexistence of both materials within the fabricated composite, validating the effectiveness of the impregnation process.

Scanning electron microscope (SEM)

image displays the microstructure of 3DP HA/PCL composite bone graft material at 50x, 100x and 500x magnification (Figures 3C,3D,3E). The micrograph reveals a complex, three-dimensional architecture composed of particles varying in size and morphology in which the HA crystals were coated or infiltrated with PCL. Particles range from sub-micron to several micrometers in diameter, exhibiting both spherical and irregular shapes. This heterogeneous particle distribution creates a highly porous structure with interconnected spaces, crucial for cellular infiltration and vascularization in bone regeneration processes.

Mechanical properties : The compressive load resistance of the 3DP HA/PCL composite granules was 7.55 ± 1.71 N. The cross-sectional area at the largest diametral area was considered, the calculated compressive strength of the granule was approximately 2.4 MPa.

MicroCT analysis : The microtomographic reconstructed image is shown in figure 3B followed by microCT structural analysis values in table 1. The pore structure of a 3DP HA/PCL composite revealed good interconnectivity from the top to bottom of the construct with total porosity of 60.67%.

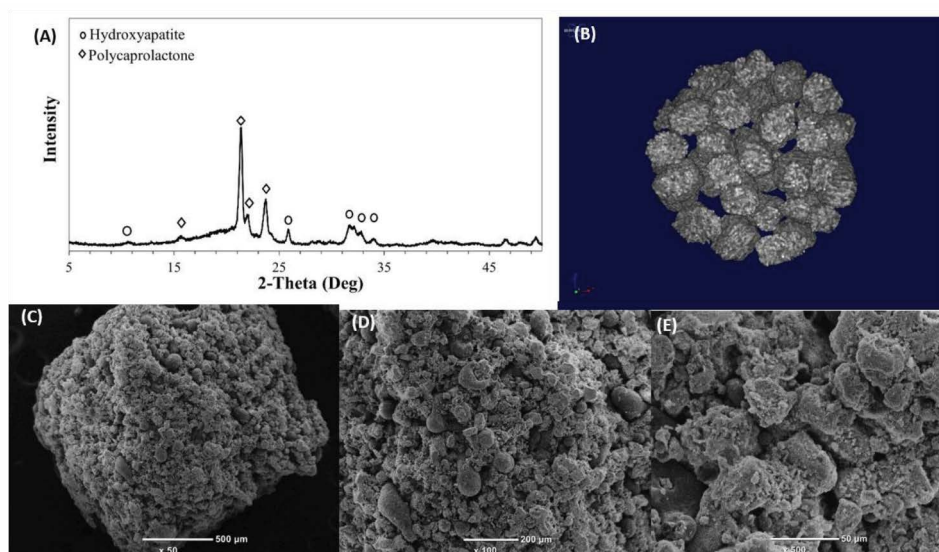


Fig.3 Characteristics of 3DP HA/PCL composite (A) XRD pattern showing characteristic peaks of both PCL and HA, confirming successful composite formation. (B) MicroCT 3D reconstructed images revealing scaffold microstructure and porosity distribution. (C-E) SEM micrographs at 50x, 100x, and 500x magnifications (scale bars: 500 μm, 200 μm, 50 μm) displaying scaffold surface topography and pore network.

Table 1. MicroCT structure analysis of the 3DP HA/PCL composite.

Description	Abbreviation	Value	Unit
Structure thickness	St.Th	0.083	mm
Structure separation	St.Sp	0.102	mm
Number of objects Obj	N	47	
Number of closed pores	Po.N(cl)	4	
Volume of closed pores	Po.V(cl)	0.00008	mm ³
Surface of closed pores	Po.S(cl)	0.015	mm ²
Closed porosity	Po	0.048	%
Open porosity	Po(op)	60.652	%
Total volume of pore space	Po.V(tot)	0.276	mm ³
Total porosity	Po(tot)	60.67	%
Connectivity	Conn	118	

Clinical evaluation:

Nineteen patients (21 maxillary sinuses) were included in this study from December 2022 to January 2024, with three patients (3 maxillary sinuses) being terminated due to lost to follow-up. Patients were randomized into control (n = 10) and test (n = 11) groups (Table 2). All patients

showed normal soft tissue and bone healing without complications such as pain, inflammation, infection, sinusitis, or other maxillary sinus pathologies throughout the follow-up period. The dental implant was successfully placed in all cases.

Table 2. Patients Demographic data and Complication.

	Control group Xenograft(10)	Test group 3DP HAPCL(11)	Total (n = 21)
Age	59 ± 8.756	52.36 ±14.22	55.52 ± 12.13
Gender			
Male	3(30)	6(54.55)	9(42.86)
Female	7(70)	5(45.45)	12(57.14)
Tooth type			
Premolar	0(0)	2(18.19)	2(9.52)
Molar	10(100)	9(81.81)	19(90.48)
Complication			
Membrane perforation	1(10)	1(9.09)	2(9.52)

No significant difference in mean Hounsfield Units (HU) was observed between the control and test groups immediately after sinus augmentation (T1) (1059 ± 104.9 HU vs. 978.1 ± 118.8 HU, p = 0.1155). However, significant differences emerged at 6 months (T2) and 12 months (T3) post-augmentation. The control group showed mean HU values of 1303 ± 213 at T2 and 1523 ± 265.7 at T3, while the test group had 1048 ± 130.5 at T2 and 1184 ± 121.6 at T3. (Table 3)

Significant differences of graft bone density in the control group across all time points (T1, T2, T3) were seen (p < 0.05). In contrast, the test group showed significant differences only between T1 and T3 (p < 0.0009) and between T2 and T3 (p < 0.0324). The percentage analysis of grafted bone density showed increasing values overtime for both control and test groups. The percentage differences between consecutive time points (T1-T2, T2-T3) and overall change (T1-T3) are shown in Table 4

Table 3. Mean grafted bone density between the control and test groups at different time points.

	Control Group (Xenograft)	Test Group (3DP HA/PCL)	P value
T1	1059 ± 104.9 ^{abc}	978.1 ± 118.8 ^{ac}	0.1155
T2	1303 ± 213.8 ^{abc}	1048 ± 130.5 ^{bc}	0.0035*
T3	1523 ± 265.7 ^{abc}	1184 ± 121.6 ^{ca}	0.0011*

Note: Mean(HU) ± standard deviation values

Abbreviations:

- Xenograft (Straumann xenograft)
- 3DP HA/PCL (polycaprolactone impregnated 3D printed hydroxyapatite)
- T1 (CBCT at immediate sinus augmentation), T2 (CBCT 6 months after sinus augmentation),
- T3 (CBCT 12 months after sinus augmentation)
- *p-values (statistically significant at the level of $p < 0.05$) with unpaired t-test for differences in HU values at each timepoint between Xenograft and 3DP HA/PCL groups.
- abc p-values (statistically significant at the level of $p < 0.05$) with ANOVA for differences within each group between T1, T2 and T3.

Table 4. Percentage increase of grafted bone density overtime between the control and test groups at different time points.

	Control Group (Xenograft)	Test Group (3DP HA/PCL)
T1-2%	23%	7%
T2-3%	17%	13%
T1-3%	44%	21%

Abbreviations:

- T1-2% Percentage increase of early grafted bone density changes
- T2-3% Percentage increase of late grafted bone density changes
- T1-3% Percentage increase of overall grafted bone density changes

Discussion

Recently, advancements in 3D printing technology combined with low-temperature phase transformation techniques have led to the development of 3DP hydroxyapatite (3DP HA) bone substitutes. These substitutes exhibit unique properties such as nanostructure, low crystallinity, resorbability, and high wicking ability, contrasting with the typically high-temperature sintered HA (21,25,26). Preclinical and clinical studies have demonstrated promising results for using this 3DP HA as a bone graft in socket preservation and bone block grafts for implant sites. (27,28) However, the mechanical strength of 3DP HA remains relatively low, potentially limiting its ability to withstand stress in certain applications. This limitation is associated with its high porosity due to calcium phosphate crystal precipitation during processing, which may present handling challenges in specific procedures (21,25,26). To address this drawback, a polycaprolactone (PCL) infiltrated 3DP HA composite (HA/PCL) was developed to enhance the toughness and strength of the material while maintaining its biocompatibility and bioactivity (18). PCL, a biodegradable polyester, was chosen as the infiltrant phase due to its favorable mechanical properties, degradability, and long history of use in implants. PCL initially provides structural integrity, which subsequently degrades to offer the porous architecture necessary for tissue ingrowth.

In this study, 3DP HA/PCL composite granules were prepared using modified and proprietary techniques to form spherical granules approximately 2 mm in diameter, suitable for use as a bone graft for maxillary augmentation. Compared to the previously investigated large rectangular bars (19), the 3DP HA/PCL composite

granules similarly exhibited a highly porous structure with interconnected spaces crucial for cellular infiltration and vascularization in bone regeneration processes, as evidenced by SEM images and micro-CT analysis. The microstructure comprises a three-dimensional architecture of HA crystals with varying sizes and morphologies, infiltrated or coated by PCL, yet retaining numerous micropores. The compressive load resistance of the 3DP HA/PCL composite granules was 7.55 ± 1.71 N. Due to the spherical shape of the granule, it was not straightforward to calculate the compressive strength. However, if the cross-sectional area at the largest diametral area was considered, the calculated compressive strength of the granule was approximately 2.4 MPa, which is about seven times greater than that of 3D HA granules alone. The compressive strength of cortical bone ranges from 100–230 MPa, while that of trabecular bone ranges from 2–12 MPa (29). The mechanical properties of 3DP HA/PCL composite granules are thus comparable to those of trabecular bone. Several studies have shown that the primary function of scaffolds is to act as structural templates that provide suitable substrates for cell proliferation, differentiation, and attachment, leading to new tissue formation. These processes depend on factors such as porosity, pore size, geometry, and interconnectivity. High porosity and large pores enhance bone ingrowth and osseointegration of the implant after surgery (30). Although the pore size of 3DP HA/PCL composite granules was not large, previous clinical studies have demonstrated that 3DP HA granules with small pore sizes can support bone regeneration through its highly porous structure and resorbability, which generate the necessary spaces for cells and bone ingrowth

during the bone healing process (26,27). It was anticipated that 3DP HA/PCL composite granules could also support bone regeneration by a similar mechanism, but can resist greater load during handling.

Bone density in dentistry is measured using CBCT images and expressed in Hounsfield Units (HU). This assessment of bone quality, crucial for predicting implant stability and prognosis, is typically categorized using Misch's classification (1988) into four groups: D1, D2, D3, and D4. This system aids clinicians in treatment planning and evaluating potential implant sites (3).

In this study, the initial mean Hounsfield Units (HU) at T1 for Xenograft and 3DP HA/PCL were 1059 ± 104.9 and 978.1 ± 118.8 , respectively, showing no significant difference. These values are comparable to D2 bone density in Misch classification (5), indicating that both materials provide a suitable initial scaffold for bone regeneration in sinus augmentation procedures. However, significant differences emerged at 6 months (T2) and 12 months (T3) post-augmentation. The Xenograft group showed higher mean HU values (T2: 1303 ± 213.8 , T3: 1523 ± 265.7) compared to the 3DP HA/PCL group (T2: 1048 ± 130.5 , T3: 1184 ± 121.6). This divergence in bone density over time suggests different patterns of bone maturation and remodeling between the two materials. The Xenograft group demonstrated a progression from D2 to D1 bone density, indicating a rapid and robust bone formation process. This improvement in bone quality could be attributed to the osteoconductive properties of xenografts and their ability to integrate well with host bone. In contrast, The 3DP HA/PCL composite showed a slower,

statistically non-significant increase in bone density from the T1 to T2 timepoints. However, it then exhibited a statistically significant accelerated rate of bone density gain between the T2 and T3 timepoints. This acceleration in bone density growth during the T2 to T3 period, while not matching the exact rate observed in the xenograft group, followed a similar overall trend of increased bone density during that time interval.

The findings were converted to percentages to facilitate a more comprehensive understanding of the results. By T3 revealed that the control group demonstrated a 44% increase in grafted bone density, compared to only 21% in the test group, suggesting superior bone formation with xenograft materials. These findings suggest that the bone healing and remodeling processes differ between Xenograft and 3DP HA/PCL materials. The Xenograft group's steady progression might be attributed to the osteoconductive properties of xenografts and their ability to integrate well with host bone (31). On the other hand, the 3DP HA/PCL group's accelerated late-phase density gain could be related to the unique properties of the 3DP HA/PCL composite fabricated from low-temperature phase transformation (24), including its biodegradation and interaction with surrounding tissues. Similar to previous study (27) that showed a healing index increased over time at 2 weeks, 1, 2, 3, and 6 months after block-graft with customized 3DP nanohydroxyapatite on implant site.

This is a preliminary report of the clinical evaluation of 3DP HA/PCL composite for maxillary sinus augmentation. Future analyses and reports should focus on correlating these bone density changes with clinical outcomes such as implant

stability, osseointegration, and long-term success rates. While bone density measurements indicated differences between groups, these results should be interpreted with caution as they cannot differentiate between new bone formation and residual graft materials. In contrast, histomorphometric analysis provides direct microscopic evidence of bone formation and is therefore more reliable for evaluating true osteogenic outcomes.

Conclusion

3DP HA/PCL composite demonstrates potential as an alternative bone graft material to deproteinized bovine bone mineral. While both deproteinized bovine bone mineral and 3DP HA/PCL composite materials demonstrate effectiveness in sinus augmentation but xenograft shows higher bone density results. However, their distinct patterns of bone density progression offer unique advantages. The choice between these materials should be based on a comprehensive consideration of the clinical scenario, patient factors, and desired timeline for implant placement.

Acknowledgements

This research was supported by Thammasat University research fund, Contract No. TUFT 93/64 and Thammasat University-National Science and Technology Development Agency Excellent Research Graduate Scholarship (T2.2-63-01). The authors would like to acknowledge the participants of the study and the staff of the Department of Implantology, Faculty of Dentistry, Thammasat University, for their assistance in conducting this clinical trial.

References

1. Berglundh T, Persson L, Klinge B. A systematic review of the incidence of biological and technical complications in implant dentistry reported in prospective longitudinal studies of at least 5 years. *J Clin Periodontol.* 2002;29(Suppl 3):197-212; discussion 32-3.
2. Schropp L, Wenzel A, Kostopoulos L, Karring T. Bone healing and soft tissue contour changes following single-tooth extraction: a clinical and radiographic 12-month prospective study. *Int J Periodontics Restorative Dent.* 2003 ;23(4):313-23.
3. Goncalves SB, Correia J, Costa AC. Evaluation of dental implants using Computed Tomography. 2013 IEEE 3rd Portuguese Meeting in Bioengineering (ENBENG). 2013:1-4. doi:10.1109/ENBENG.2013.6518387.
4. Boyne PJ, James RA. Grafting of the maxillary sinus floor with autogenous marrow and bone. *J Oral Surg.* 1980;38(8):613-6.
5. Misch CE. Maxillary sinus augmentation for endosteal implants: organized alternative treatment plans. *Int J Oral Implantol.* 1987;4(2):49-58.
6. Danesh-Sani SA, Loomer PM, Wallace SS. A comprehensive clinical review of maxillary sinus floor elevation: anatomy, techniques, biomaterials and complications. *Br J Oral Maxillofac Surg.* 2016;54(7):724-30.
7. Lie SAN, Claessen RMMA, Leung CAW, Merten HA, Kessler PAWH. Non-grafted versus grafted sinus lift procedures for implantation in the atrophic maxilla: a systematic review and meta-analysis of randomized controlled trials. *Int J Oral Maxillofac Surg.* 2022;51(1):122-32.

8. Rickert D, Slater JJRH, Meijer HJA, Vissink A, Raghoobar GM. Maxillary sinus lift with solely autogenous bone compared to a combination of autogenous bone and growth factors or (solely) bone substitutes. a systematic review. *Int J Oral Maxillofac Surg.* 2012;41(2):160-7.
9. Cardoso CL, Curra C, Santos PL, Rodrigues MFM, Ferreira-Júnior O, de Carvalho PSP. Current considerations on bone substitutes in maxillary sinus lifting. *Revista Clínica de Periodoncia, Implantología y Rehabilitación Oral.* 2016;9(2):102-7.
10. Ginebra MP, Espanol M, Maazouz Y, Bergez V, Pastorino D. Bioceramics and bone healing. *EFORT Open Rev.* 2018;3(5):173-83.
11. Kattimani VS, Kondaka S, Lingamaneni KP. Hydroxyapatite--Past, Present, and Future in Bone Regeneration. *Bone and Tissue Regeneration Insights.* 2016;7. doi:10.4137/BTRI.S36138
12. Zhao R, Xie P, Zhang K, Tang Z, Chen X, Zhu X, et al. Selective effect of hydroxyapatite nanoparticles on osteoporotic and healthy bone formation correlates with intracellular calcium homeostasis regulation. *Acta Biomater.* 2017;59:338-50. doi: 10.1016/j.actbio.2017.07.009.
13. LeGeros RZ. Calcium phosphate-based osteoinductive materials. *Chem Rev.* 2008;108(11):4742-53.
14. Zhiwei J, Bin L, Shengyi X, Haopeng M, Yuan Y, Weimin Y. 3D printing of HA / PCL composite tissue engineering scaffolds. *Advanced Industrial and Engineering Polymer Research.* 2019;2(4):196-202.
15. Stevanovic S, Chavanne P, Braissant O, Pieleas U, Gruner P, Schumacher R. Improvement of mechanical properties of 3d printed hydroxyapatite scaffolds by polymeric infiltration. *Bioceram. Dev. Appl.* 2013;3:10-2. doi: 10.4172/2090-5025.S1-012.
16. Kim BS, Yang SS, Park H, Lee SH, Cho YS, Lee J. Improvement of mechanical strength and osteogenic potential of calcium sulfate-based hydroxyapatite 3-dimensional printed scaffolds by ϵ -polycarbonate coating. *J Biomater Sci Polym Ed.* 2017;28(13):1256-70.
17. BaoLin G, Ma PX. Synthetic biodegradable functional polymers for tissue engineering: a brief review. *Sci China Chem.* 2014;57(4):490-500.
18. Taecha-Apaikun K, Pisek P, Suwanprateeb J, Thammarakcharoen F, Arayatrakoolikit U, Angwarawong T, et al. In vitro resorbability and granular characteristics of 3D-printed hydroxyapatite granules versus allograft, xenograft, and alloplast for alveolar cleft surgery applications. *Proc Inst Mech Eng H.* 2021;235(11):1288-96.
19. Suwanprateeb J, Thammarakcharoen F, Hobang N. Enhancement of Mechanical Properties of 3D printed Hydroxyapatite by Combined Low and High Molecular Weight Polycaprolactone Sequential Infiltration. *J. Mater. Sci.* 570 Mater. Med. 2016;27(11):171. doi: 10.1007/s10856-016-5784-4.
20. Hemstapat R, Suwanprateeb J, Sriwatananukulkit O, Luangwattanawilai T, Desclaux SS. Study of bone regeneration of a porous hydroxyapatite scaffolds infiltrated with polycaprolactone and polycaprolactone membrane in a rat model. [Study report: Sponsored by the National Metal and Materials Technology Center] Bangkok: Department of Pharmacology, Mahidol University; 2019.

21. Suwanprateeb J, Thammarakcharoen F, Wasoontarat K, Suvannapruk W. Influence of printing parameters on the transformation efficiency of 3D-printed plaster of paris to hydroxyapatite and its properties. *Rapid Prototyping J.* 2012;18(6):490-9.
22. Kijartorn P, Thammarakcharoen F, Suwanprateeb J, Buranawat B. The use of three dimensional printed hydroxyapatite granules in alveolar ridge preservation. *Key Eng Mater.* 2017;751:663-7. doi:10.4028/www.scientific.net/KEM.751.663.
23. Thammarakcharoen F, Suwanprateeb J. Effect of process parameters on biomimetic deposition of calcium phosphate on 3D printed hydroxyapatite. *Key Eng Mater.* 2017;751:599-604.
24. Julious SA. Sample size of 12 per group rule of thumb for a pilot study. *Pharmaceutical Statistics.* 2005;4(4):287-91.
25. Suwanprateeb J, Suvannapruk W, Wasoontarat K. Low temperature preparation of calcium phosphate structure via phosphorization of 3D-printed calcium sulfate hemihydrate based material. *J Mater Sci Mater Med.* 2010;21(2):419-29.
26. Kijartorn P, Wongpairojpanich J, Thammarakcharoen F, Suwanprateeb J, Buranawat B. Clinical evaluation of 3D printed nano-porous hydroxyapatite bone graft for alveolar ridge preservation: A randomized controlled trial. *J Dent Sci.* 2022;17(1):194-203.
27. Mekcha P, Wongpairojpanich J, Thammarakcharoen F, Suwanprateeb J, Buranawat B. Customized 3D printed nanohydroxyapatite bone block grafts for implant sites: A case series. *J Prosthodont Res.* 2023;67(2):311-320.
28. Suwanprateeb J, Thammarakcharoen F, Hobang N. Enhancement of mechanical properties of 3D printed hydroxyapatite by combined low and high molecular weight polycaprolactone sequential infiltration. *J Mater Sci Mater Med.* 2016;27(11):171. doi:10.1007/s10856-016-5784-4.
29. Loh QL, Choong C. Three-dimensional scaffolds for tissue engineering applications: role of porosity and pore size. *Tissue Eng Part B Rev.* 2013;19(6):485-502.
30. Karageorgiou V, Kaplan D. Porosity of 3D biomaterial scaffolds and osteogenesis. *Biomaterials.* 2005;26(27):5474-91.
31. Ferraz MP. Bone Grafts in Dental Medicine: An Overview of Autografts, Allografts and Synthetic Materials. *Materials (Basel).* 2023;16(11):4117. doi: 10.3390/ma16114117.

Corresponding author:

Assoc.Prof.Dr. Borvornwut Buranawat
Research Unit in Innovations in Periodontics,
Oral Surgery and advanced technology in
Implant Dentistry, Faculty of Dentistry,
Thammasat University, Pathum Thani, 12120,
Thailand
Tel: (668) 5997 7669
E-mail: borvornw@tu.ac.th